On Vibrational Circular Dichroism Chirality Transfer in Electron Donor–Acceptor Complexes: A Prediction for the Quinine · · · BF3 System. J Phys Chem A 116:7916

ARTICLE *in* THE JOURNAL OF PHYSICAL CHEMISTRY A · JULY 2012

Impact Factor: 2.69 · DOI: 10.1021/jp304955v · Source: PubMed

THE JOURNAL OF PHYSICAL CHEMISTRY A

Article

pubs.acs.org/JPCA

On Vibrational Circular Dichroism Chirality Transfer in Electron Donor−Acceptor Complexes: A Prediction for the Quinine···BF_3 System

Joanna E. Rode,*[,†] Michał H. Jamróz,[†] Jan Cz. Dobrowolski,[†,‡] and Joanna Sadlej[‡,§]

[†]Industrial Chemistry Research Institute, 8 Rydygiera Street, 01-793 Warsaw, Poland

[‡]National Medicines Institute, 30/34 Chełmska Street, 00-725 Warsaw, Poland

[§] Faculty of Chemistry, Warsaw University, 1 Pasteura Street, 02-093 Warsaw, Poland

Supporting Information

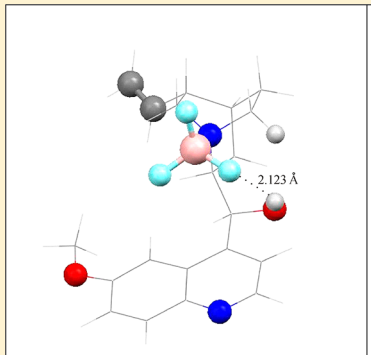

The most stable quinine···BF_3 EDA complex.

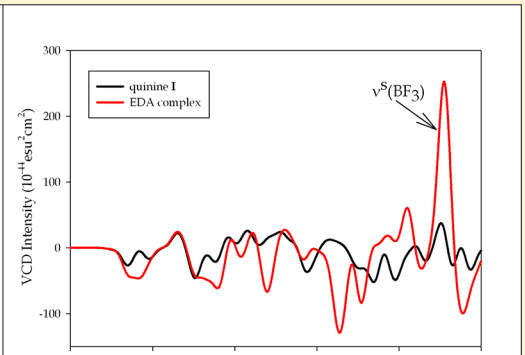

The diagnostic VCD chirality transfer band of the EDA complex.

ABSTRACT: Vibrational circular dichroism (VCD) chirality transfer occurs when an achiral molecule interacts with a chiral one and becomes VCD-active. Unlike for H-bonds, for organic electron donor−acceptor (EDA) complexes this phenomenon remains almost unknown. Here, the VCD chirality transfer from chiral quinine to achiral BF_3 is studied at the B3LYP/aug-cc-pVDZ level. Accessibility of four quinine electron donor sites changes with conformation. Therefore, the quinine conformational landscape was explored and a considerable agreement between X-ray and the most stable conformer geometries was achieved. The BF_3 complex through the aliphatic quinuclidine N atom is definitely dominating and is predicted to be easily recognizable in the VCD spectrum. Out of several VCD chirality transfer modes, the $\nu^s(BF_3)$ mode, the most intense in the entire VCD spectrum, satisfies the VCD mode robustness criterion and can be used for monitoring the chirality transfer phenomenon in quinine···BF_3 system.

1. INTRODUCTION

The vibrational circular dichroism (VCD) technique, known since the mid-1970s,[1−4] is a difference of vibrational spectra taken with respect to left versus right circularly polarized IR light. The VCD bands are ca. 10^4−10^6 times less intense than IR bands; however, occasionally some very strong VCD bands, of intensity comparable with those in the IR spectra, were predicted.[5] In contrast to IR, VCD spectroscopy discriminates individual enantiomers and enables studies on optically active molecules.[6,7] Enantiomers are mirror images in the 3D space, while their VCD spectra are mirror images against the wavenumber axis. VCD is superior to electronic circular dichroism (ECD) in identifying the molecular moieties of the studied systems. Indeed, a large number of bands is present in the VCD spectrum of a chiral substance while only a few broad ones are usually present in the ECD spectrum. Also, the calculated VCD spectra are more reliable than the ECD ones, because of difficulties in adequate consideration of the role of excited electronic states in the ECD phenomenon.[8] On the other hand, the ECD/UV−vis intensity ratio is usually much greater than the VCD/IR ratio, and the ECD method is more sensitive to a chiral substance. Nevertheless, VCD experiments accompanied by quantum chemical calculations can serve as an elegant technique for determining the absolute configuration.[9−15]

VCD spectra have been shown to exhibit potential in studies of intermolecular complexes. The insight into intermolecular interaction phenomena is especially sophisticated when a chiral

Received: May 22, 2012
Revised: July 4, 2012
Published: July 5, 2012

molecule interacts with an achiral one. In such a case, an achiral molecule, that is transparent in VCD when not perturbed, becomes VCD-visible in the presence of a chiral one.[16,17] This phenomenon is called chirality transfer or induced chirality. VCD chirality transfer was probably first observed in 2002, for the ν(C═O) band of trifluoroacetic acid forming an H-bond complex with cinchonidines.[18] The authors suggested the "induced VCD" effect would allow probing of the chiral binding site. In 2003 we published a study on VCD spectra of intermolecular H-bonding complexes of model chiral β-lactams with HX molecules (X = F, Cl, Br).[19] We stressed that achiral HX molecules interacting with chiral molecules gained significant VCD rotational strength and the sign revealed the geometry of the hydrogen bond. Next, we studied VCD spectra of H-bond D-lactic acid−water[20] and cysteine−water[21] complexes, which despite clear chirality transfer phenomena exhibited a rich conformational changeability, making interpretation much more knotty.

Nowadays, there are more experimental and theoretical studies demonstrating the VCD chirality transfer phenomenon to be a promising tool in investigations of intermolecular interactions.[22−31] There are also publications of chirality transfer observed in matrix-isolated (MI) VCD experiments. Studies on a peptide−water complex registered in Ar matrix showed that transitions of the achiral water molecule could be identified in both MI and solution VCD spectra.[32] It is also shown that the signs of these transitions were sensitive to the alignment of the complexed water and could be used for structural identification of the complexes.[32]

Until very recently, experimental and theoretical VCD studies reporting chirality transfer phenomena were devoted to intermolecular systems interacting via H-bonds. However, except the hydrogen bonds, the directional intermolecular electron donor−acceptor (EDA) interactions, also called charge-transfer interactions, play a fundamental role in organizing the chemical and biochemical systems. The EDA interactions occur between electron-deficient centers and electron-rich ones (e.g., BF_3, BCl_3, tetracyanoethylene, CO_2, etc., and free electron pairs or π-electrons of aromatic rings, respectively). For example, EDA interactions shape peptide conformations by interactions of amino acid aromatic side chains. Analogously, they play an essential role in drug−receptor recognition[33,34] and in many other fields.[35−38] The VCD chirality transfer in electron donor−acceptor (EDA) complexes has first been studied in our recent study on sulfinimine−BF_3 complex.[39]

The EDA interaction was first and foremost studied by UV−vis spectroscopy[40,41] but it can be also observed in the IR range[42−45] or by rotational spectroscopy[46] or NMR.[47] The appearance of a new absorption band (electronic or vibrational), not attributable to separate complex components, often is taken as evidence for charge transfer in EDA interactions. In our recent paper,[39] we have shown that, in the sulfinimine−BF_3 complex, VCD chirality transfer can be observed for these very EDA complexes and that this fact can be helpful in judging which sulfinimine electron-donating center is mostly engaged in the complex.

Here, we continue investigating the VCD chirality transfer phenomenon in intermolecular EDA complexes. The EDA complex of chiral quinine and achiral BF_3 was chosen for several reasons: (i) quinine is widely used and has four different electron donor sites, (ii) BF_3 is a very active electron acceptor forming quite strong EDA complexes, and (iii) the quinine···BF_3 system can be a zero-approximation reference system for quinine EDA complexes with weaker electron acceptors such as carbon dioxide.

Quinine (Scheme 1) belongs to cinchona alkaloids (widely used in the pharmaceutical and chemical industry)[48] and

Scheme 1. Quinine

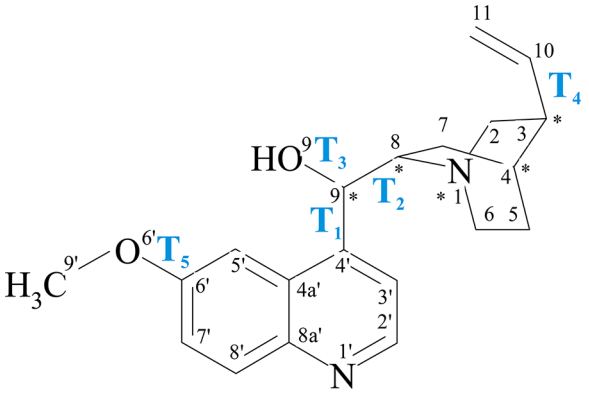

contains two major fused-ring systems, the aromatic quinoline and the aliphatic quinuclidine, connected through the -CH-(OH)- linkage. Four electron-donating sites of quinine are available for the electron-deficient moiety: two nitrogen atoms in the two rings, and two oxygen atoms of the alcohol and methoxy groups (Scheme 1). Quinine is used, inter alia, as an enantioselective reagent, yet possibly the most important application of quinine, and the other cinchona alkaloids, in chemistry resides in their ability to promote enantioselective transformations in both homogeneous and heterogeneous catalyzes.[48] Quinine has also found extensive use as a resolving agent for racemic chiral (Lewis) acids.[49] However, most of the chiral separation methods are expensive, need vast quantities of organic solvent, and involve time-consuming crystallization or chromatographic separations hardly acceptable by modern technological requirements. Therefore, use of supercritical CO_2 with enantiomer-resolving agents, such as quinine modified by a substituent increasing solubility in the fluid phase, offers an attractive alternative to traditional organic media.[50] It would be desirable to have a chiral-sensitive method capable of monitoring the interactions in the system, and in this respect the VCD method seems to be an interesting technique. Yet the EDA interactions with CO_2, as a solvent, are relatively weak; therefore, we decided to analyze much stronger complexes of quinine with BF_3 to check whether such interactions can be successfully detected and monitored by the VCD method or not.

The aim of this study has been examination of the features of the VCD chirality transfer phenomenon in the case of relatively strong EDA complexes. In contrast to the classical methods of vibrational IR and Raman spectroscopy, for which the canonical behavior of the bands upon H-bond and EDA complex formation is very well recognized,[51] the behavior of the VCD intensities upon complexation remains unknown. At the moment no rule has been proposed about magnitude or sign of the band related to complex formation. Especially, the chirality transfer bands, exclusively present in chiroptical spectroscopy, require more study. The present study shows analysis of the VCD chirality bands in the case of the quinine···BF_3 complex model, which ought to be verifiable experimentally.

dx.doi.org/10.1021/jp304955v | J. Phys. Chem. A 2012, 116, 7916−7926

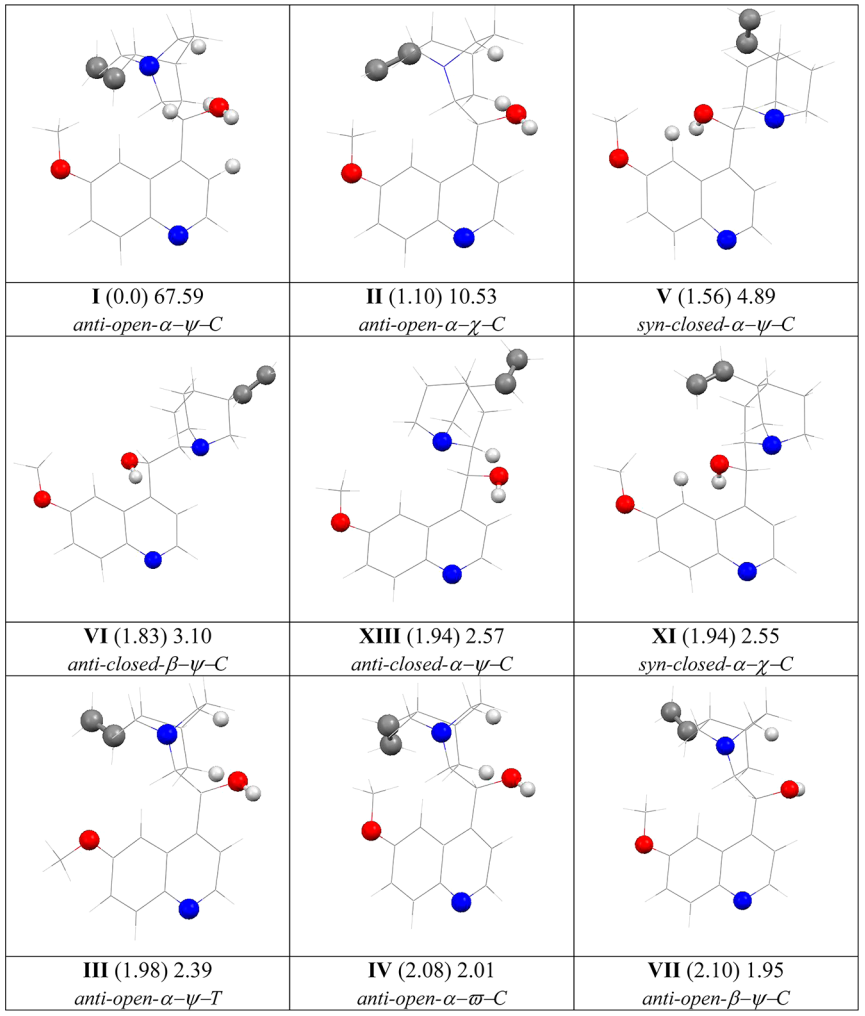

Figure 1. B3LYP/aug-cc-pVDZ nine most populated quinine conformers relative to the most stable conformer. There are ΔG energies (kilocalories per mole) in parentheses and populations (percentages) based on the ΔG values, respectively. Heavy atoms and hydrogen atoms that could form intermolecular hydrogen bonds are exposed only for clarity.

The paper is organized as follows: First, the conformational landscape of quinine is analyzed. Second, the four most stable quinine EDA complexes with BF_3 are selected and discussed. Third, the VCD spectra of these complexes are analyzed. Fourth, the robustness of the VCD chirality transfer signals is checked and concluded.

2. COMPUTATIONAL DETAILS

All the calculations were performed by using the hybrid Becke three-parameter Lee–Yang–Parr density functional theory (DFT) B3LYP functional,[52,53] whose reliability in calculations of the ground-state geometries has been widely assessed.[54] The cc-pVDZ[55] basis set was used for optimization of all 67 quinine conformers, whereas the aug-cc-pVDZ Dunning's[56] basis set was employed for the 15 most stable quinine structures and for intermolecular quinine···BF_3 complexes. Especially, the augmented basis sets are known to be adequate in describing both organic molecules and their intermolecular interactions. The conformational space of quinine was explored through a systematic rotation about the single bonds by changing the following five dihedrals: T_1 ($C^{4a'}$–$C^{4'}$–C^9–C^8), T_2 ($C^{4'}$–C^9–C^8–N^1), T_3 (H–O^9–C^9–$C^{4'}$), T_4 (C^2–C^3–C^{10}–C^{11}), and T_5 ($C^{5'}$–$C^{6'}$–$O^{6'}$–C^9), where primes denote atoms in the aromatic quinoline ring (Scheme 1). Optimization of the local minima was confirmed by ascertaining that all the harmonic frequencies were real. The conformers were ordered according to the increasing total energy obtained at the B3LYP/cc-pVDZ level. The conformer population of 67 quinine local minima found was calculated by use of a Boltzmann distribution at normal conditions and ΔG Gibbs free energy differences calculated at the B3LYP/cc-pVDZ level.

The interaction energies were corrected by the counterpoise method[57] and seven-point correction method for basis-set superposition error[58] (BSSE) as described in ref 59. The seven-point description of BSSE interaction energy includes the deformation energy of the complex partners.[59]

All the calculations were performed by using the Gaussian 09 package of programs.[60] For the calculated harmonic spectra, the potential energy distribution (PED) analysis of normal modes have been performed by using the VEDA (vibrational energy distribution analysis) program.[61] In PED analysis, the normal mode coordinates are expressed in terms of internal mode coordinates. Each of the internal coordinates is next expressed as a superposition of several local modes of two, three, or four atoms connected by bonds. Detailed methodology of the PED analysis can be found in refs 62–66.

dx.doi.org/10.1021/jp304955v | J. Phys. Chem. A 2012, 116, 7916–7926

Table 1. Main Dihedral Angles in the Nine Most Populated Quinine Conformers[a]

	G(X), %	T_1, deg	T_2, deg	T_3, deg	T_4, deg	T_5, deg	geometry class
I	67.59	−79.3	153.4	−62.1	121.5	−0.1	*anti open* α−ψ−C
II	10.53	−79.5	151.0	−61.2	5.3	−0.5	*anti open* α−χ−C
III	2.39	−79.5	155.4	−63.2	121.2	−179.7	*anti open* α−ψ−T
IV	2.01	−79.1	150.0	−61.3	−134.7	−0.6	*anti open* α−ω−C
V	4.89	70.0	54.8	−52.5	121.5	0.0	*syn closed* α−ψ−C
VI	3.10	−166.9	55.7	47.4	120.3	−0.2	*anti closed* β−ψ−C
VII	1.95	−73.8	151.2	68.8	121.0	−0.8	*anti open* β−ψ−C
XI	2.55	69.9	56.7	−51.8	6.5	0.1	*syn closed* α−χ−C
XIII	2.57	−111.3	60.4	−51.8	121.3	0.0	*anti closed* α−ψ−C

[a]Calculated at the B3LYP/aug-cc-pVDZ level.

Table 2. Main Dihedral Angles in Quinine Conformer I[a] and Available Experimental X-ray Data

	this study	X-ray structures				semiempirical
angle[b]	conformer **I** *anti open* α	KAMDAD[77] *anti open* α	LIQBAP[73] *anti open* γ	DADCUG[74] *anti open* α	MOHBOA[75] *anti open* α	PM3[72] *anti closed* α
T_1, deg	−79.3	−71.9	−74.7	−79.9	−86.0	−114.3
T_2, deg	153.4	147.4	167.7	165.0	165.1	67.6
T_3, deg	−62.1	−77.4	−127.0	−75.4	−72.2	−65.4
T_4, deg	121.5	127.4	11.9			100.8
T_5, deg	−0.1	8.1	4.8	−2.2	4.02	0.9

[a]Calculated at the B3LYP/aug-cc-pVDZ level. [b]T_1= $C^{4a\prime}$−$C^{4\prime}$−C^9−C^8; T_2 = $C^{4\prime}$−C^9−C^8−N^1; T_3 = H−O^9−C^9−$C^{4\prime}$; T_4 = C^2−C^3−C^{10}−C^{11}; T_5 = $C^{5\prime}$−$C^{6\prime}$−$O^{6\prime}$−$C^{9\prime}$. Atom labeling is shown in Scheme 1.

3. RESULTS AND DISCUSSION

3.1. Conformation and Energetics of Quinine. The quinine molecule has five single bonds around which free rotations may lead to as much as 243 local minima. To generate quinine conformers, the relevant torsion angles T_1−T_5 (see Computational Details) were varied systematically at the semiempirical AM1 level, yielding ca. 100 stable quinine conformers, which after reoptimization at the B3LYP/cc-pVDZ level yielded 67 stable structures (Table 1SI, Supporting Information). The conformer population at 298 K indicates the 14 most stable conformers (**1**−**11** and **13**−**15**) accounted for 96.5% of the mixture. Next, the 14 conformers reoptimized at the B3LYP/aug-cc-pVDZ level fall into the energy interval of only 3 kcal/mol (Table 2SI, Supporting Information). However, only nine of them were populated at more than 1%, and these nine conformers were chosen for further studies (Figure 1). For the Cartesian coordinates of the nine most stable quinine conformers found at the B3LYP/aug-cc-pVDZ level, see Table 3SI in Supporting Information.

The conformational landscape of some cinchona alkaloids was studied by both spectroscopic and computational methods.[67−71] Dijkstra et al.[68,69] were probably the first who investigated the conformational behavior of quinine by means of NMR spectroscopy supported by molecular mechanics calculations. They found that the rotations about the C^8−C^9 and $C^{4\prime}$−C^9 bonds were crucial in determining four principal types of conformations: *syn-closed*, *syn-open*, *anti-closed*, and *anti-open*.[68,69] A comprehensive study on the conformational space of the cinchona alkaloids was performed in 2003 by Caner et al.[72] at the PM3 semiempirical level. The structures were systematized in terms of *syn/anti*, *open/closed/hindered*, and α/β/γ conformations. Special emphasis was given to the torsion angles T_1 ($C^{4a\prime}$−$C^{4\prime}$−C^9−C^8), T_2 ($C^{4\prime}$−C^9−C^8−N^1), and T_3 (H−O^9−C^9−$C^{4\prime}$) defining conformation of the backbone and the hydroxy group. The *syn* and *anti* conformations refer to arrangement of the methoxy and hydroxy groups against half-space determined by the plane perpendicular to the quinoline system and containing the $C^{4\prime}$−C^9 bond: in the *syn* conformation they are at the same side of the plane ($0° < T_1 < +180°$), whereas in the *anti* one they are at the opposite sides ($0° > T > −180°$).[72] The *open*, *closed*, and *hindered* conformations are defined according to rotations about the C^9−C^8 bond and refer to mutual orientation of the two N atoms connected with the T_2 torsion angle. In the *open* conformation, the quinuclidine nitrogen N^1 is away from the quinoline moiety ($120° < T_2 < 240°$); in the *closed* conformation, the lone pair of N^1 points over the quinoline moiety ($0° < T_2 < 120°$); and in the *hindered* conformation, the two ring systems are on top of each other ($0° > T_2 > −120°$). The conformation of the OH group is defined through the T_3 torsion angle equal to α, β, and γ falling into $0° > T_3 > −120°$, $0° < T_3 < 120°$, and $120° < T_3 < 240°$ intervals, respectively.[72] The T_4 and T_5 angles (Scheme 1) have not been systematized so far.[72] According to our findings, the T_4 angle, defining position of the vinyl group falls into three intervals ($0° > T_4 > 10°$, $120° > T_4 > 125°$, and $−130° > T_4 > −140°$), which we call χ, ψ, and ω, respectively. On the other hand, the T_5 angle, defining position of the methoxy group, adopts two values around 0° and 180°, and thus we call the conformations *C* and *T*, respectively. The T_1−T_5 dihedral angles of the nine most populated quinine conformers are gathered in Table 1, and the structures are illustrated in Figure 1. Notice that the most stable two forms, **I** and **II**, differ only by the arrangement of the vinyl moiety, that is, the T_4 angle.

Now, let us compare X-ray geometries of the four quinine derivatives/complexes[73−77] with the structure of the most stable quinine conformer **I** calculated at the B3LYP/aug-cc-pVDZ level. The molecular structure of quinine itself was not determined by crystallographic methods, thus the comparison can be done either for its quinoline $N^{1\prime}$-substituted derivative (LIQBAP[73]), vinyl-group-substituted derivatives (DADCUG,[74] MOHBOA[75]), quinine-carbon-coupled dimer (JS7[76]), or

dx.doi.org/10.1021/jp304955v | J. Phys. Chem. A 2012, 116, 7916−7926

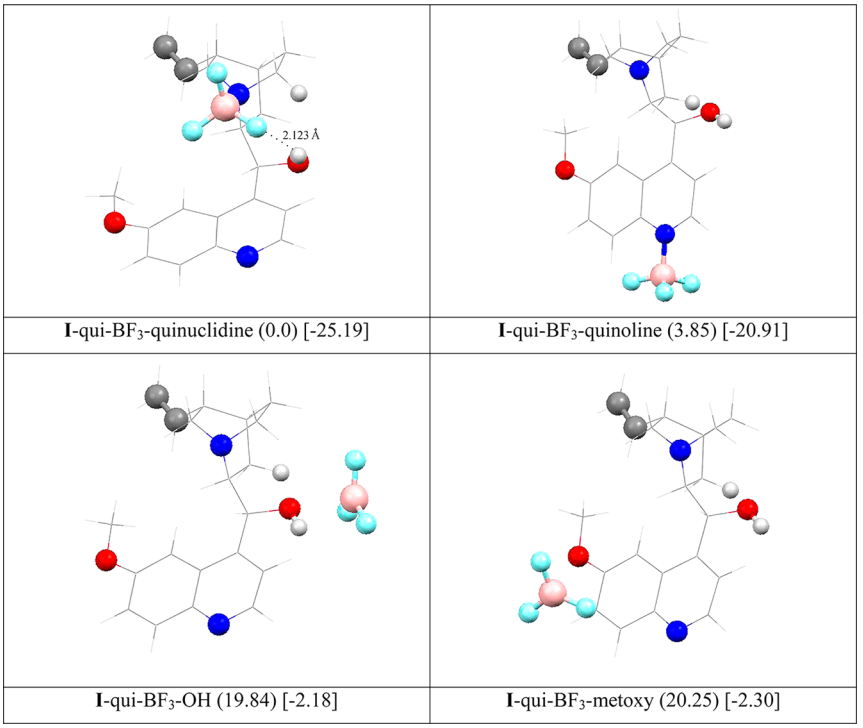

Figure 2. B3LYP/aug-cc-pVDZ optimized quinine···BF_3 complexes. The ΔG values, relative to the most stable complex, and interaction energies ΔE_7 (kilocalories per mole) are shown in parentheses and brackets, respectively.

Table 3. Energetics of the Quinine···BF_3 Complex[a]

	complex energy				interaction energy				
system	ΔG kcal/mol	$X(G)$ %	ΔE kcal/mol	ΔE_0 kcal/mol	ΔE_7 kcal/mol	ΔE_{int} kcal/mol	ΔE_{CP} kcal/mol	ΔE_{def} kcal/mol	BSSE kcal/mol
I-qui-BF_3-quinuclidine	0.00	99.85	0.00	0.00	−25.19	−30.53	−63.07	37.88	−5.34
I-qui-BF_3-quinoline	3.85	0.15	6.10	5.35	−20.91	−24.41	−52.09	31.19	−3.51
I-qui-BF_3-OH	19.84	0.00	25.78	23.84	−2.18	−4.77	−3.82	1.64	−2.59
I-qui-BF_3-methoxy	20.25	0.00	26.21	24.24	−2.30	−4.26	−3.65	1.35	−1.97

[a]Calculated at the B3LYP/aug-cc-pVDZ level. Shown are total energies (ΔE), total energies corrected for zero-point energies (ΔE_0) and Gibbs free energies at 298.15 K (ΔG), referred to the most stable complex, population [$X(G)$, %] based on the ΔG values. Interaction energies (ΔE_{int}), interaction energies corrected for BSSE by counterpoise (ΔE_{CP}) and seven-point methods (ΔE_7), deformation energies (ΔE_{def}), and BSSE error as $\Delta E_{int} - \Delta E_7$ are also shown.

quinine complexed with water and toluene (KAMDAD[77]). The comparison summarized in Table 2 shows unequivocally that conformation of the calculated conformer **I** fits very well to that of quinine complex with water and toluene.[77] It is striking that, similarly to the conformation of conformer **I**, all the molecular quinine structure in crystals, but quinoline $N^{1'}$-substituted derivative,[73] are in the *anti open* α configuration, while the PM3-optimized one is in the *anti closed* α,[72] showing that this very semiempirical method is inappropriate for prediction of the conformational landscape of quinine (Table 2). Let us add that the largest discrepancy between conformer **I** and quinine complexed with water and toluene is in T_3 torsion, changed in the experiment by the H-bond with water molecule.[77] Finally, the very good reproduction of the experimental geometry by conformer **I** can be confirmed by comparison of the remaining geometrical parameters presented in Table 4SI in Supporting Information.

3.2. Energetics and Geometry of Quinine···BF_3 Complexes. Quinine possesses four basic sites available for acids: two nitrogen atoms in the aromatic quinoline and aliphatic quinuclidine rings, and two oxygen atoms of the alcohol and methoxy groups (Scheme 1). Four principal intermolecular quinine(**I**)···BF_3 complexes were found for the most stable quinine conformer **I** (Figure 2). Hereafter, they are denoted as I-qui-BF_3 with additional specification of the complexation site. For Cartesian coordinates of the studied systems see Table 5SI in Supporting Information.

The complexes interacting via the N atoms are more stable than those via the O atoms by ca. 20 kcal/mol (Figure 2, Table 3). As expected, the complex formed through the tertiary aliphatic quinuclidine N atom is more stable by ca. 4−6 kcal/mol than that formed through the aromatic quinoline N atom. The complexes are almost as flexible as quinine molecule itself. Therefore, we checked whether the most stable complex adopts the most preferred conformation. It appeared that indeed the most stable conformer of the most stable complex was found (Figure 1SI and Table 6SI, Supporting Information). Interestingly, two of nine complexes found at the B3LYP/cc-pVDZ level converged to the most stable I-qui-BF_3-quinuclidine one when the aug-cc-pVDZ basis set was applied. All quinine conformers of complexes formed through the quinuclidine N atom adopt the *open* conformation ($150° < T_2 < 175°$; Table

dx.doi.org/10.1021/jp304955v | J. Phys. Chem. A 2012, 116, 7916−7926

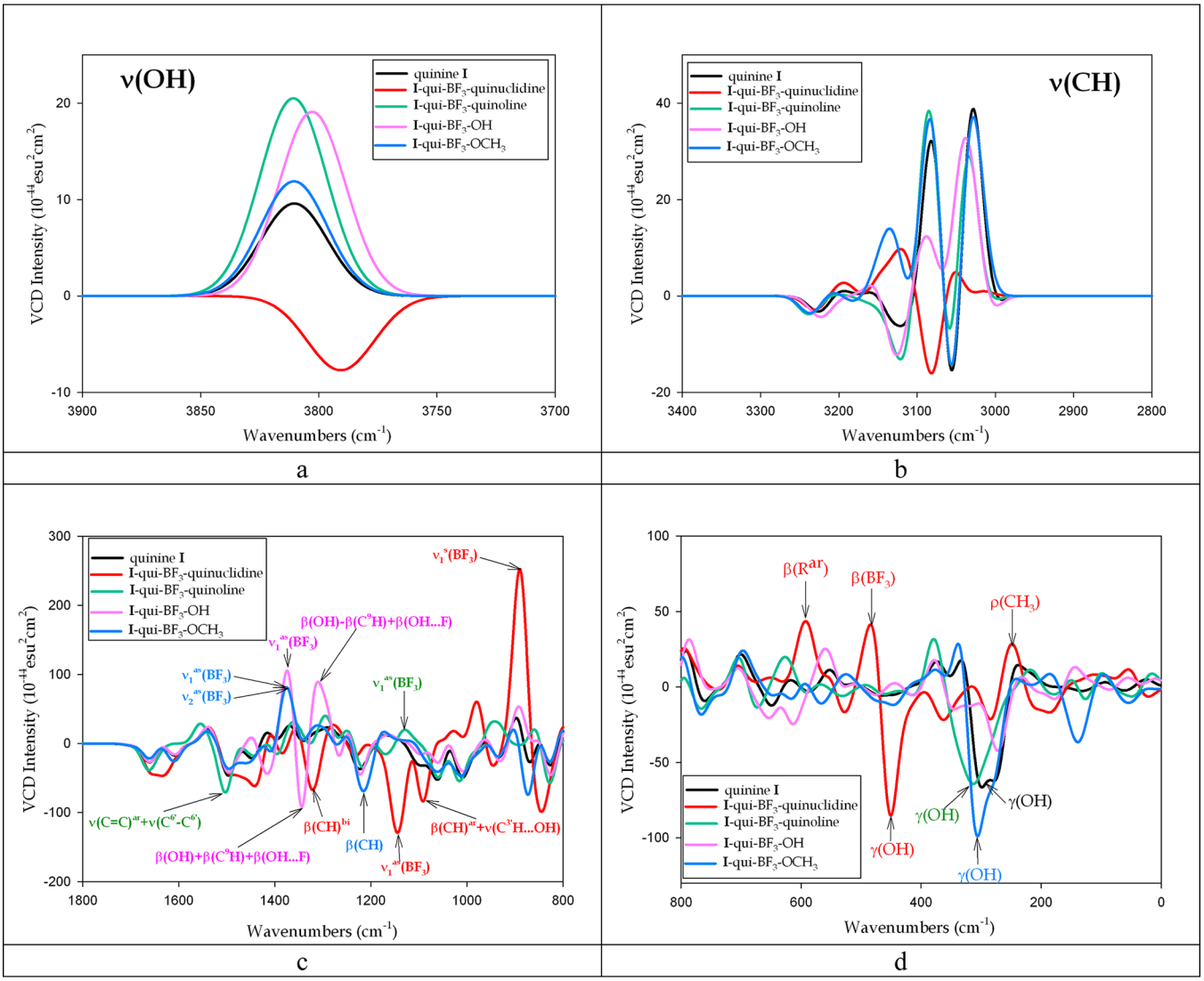

Figure 3. Population-unweighed B3LYP/aug-cc-pVDZ VCD spectra of quinine conformer **I** and its complexes with the BF_3 molecule.

6SI, Supporting Information). The *syn/anti* conformation is preserved after complexation with BF_3 (T_1 varies within ca. 20°), T_3 varies as various H-bonds of the OH group are formed with complexation, whereas the T_4 and T_5 dihedrals are constant.

Before going into details of energetics, let us recall that values obtained at the DFT level are only approximative. Indeed, much better estimation of energetics can be done by including electron correlation effects in a more explicit way, as given in perturbational or post-Hartree−Fock methods. In our studies on IR spectra of matrix-isolated amino acids (cysteine,[78] *β*-alanine,[79] and iso-serine[80]), the better electron correlation was included, the better the conformational complexity of the spectra was reproduced. For the systems studied here, calculations going beyond DFT methods are hardly possible, and thus the energetic comparisons must be treated with caution and reserve. Therefore, in the first approximation we estimated population of the four types of complexes (formed through two N and two O atoms) by using only the most stable forms of each complexation type. This estimated Boltzmann population (based on the ΔG values) shows that the **I**-qui-BF_3-quinuclidine complex is predicted to be definitely dominating in the mixture (Table 3).

The evaluation of interaction energies of the quinine···BF_3 complexes requires consideration of basis-set superposition errors. Moreover, inspection of Table 3 shows that classical counterpoise correction (ΔE_{CP})[57] yields untrustable estimation of the error because of the great destabilizing contribution of the deformation energy into the interaction energy. Therefore, here, the stabilization energy is calculated by the seven-point method (ΔE_7) including both counterpoise correction and deformation energy.[58,59] According to ΔE_7 values, **I**-qui-BF_3-quinuclidine is stabilized by ca. −25 kcal/mol and **I**-qui-BF_3-quinoline by ca. −21 kcal/mol, whereas the complexes formed through O atoms are stabilized by less than −2.5 kcal/mol (Table 3).

Note that the stabilization energy is in line with the intermolecular X···B distance equal to 1.642 Å (**I**-qui-BF_3-quinuclidine), 1.651 Å (**I**-qui-BF_3-quinoline), 2.415 Å (**I**-qui-BF_3-OH), and 2.430 Å (**I**-qui-BF_3-methoxy), respectively. It is also worth noticing that BF_3 in complexes formed through the quinine N atoms is strongly pyramidal, while in those formed through the O atoms is practically flat and similar to the trigonal planar D_{3h} symmetry of the isolated BF_3 moiety. On the contrary, the quinine moiety is perturbed relatively little, except the d(C4′−C−O−H) dihedral in the **I**-qui-BF_3-

dx.doi.org/10.1021/jp304955v | J. Phys. Chem. A 2012, 116, 7916−7926

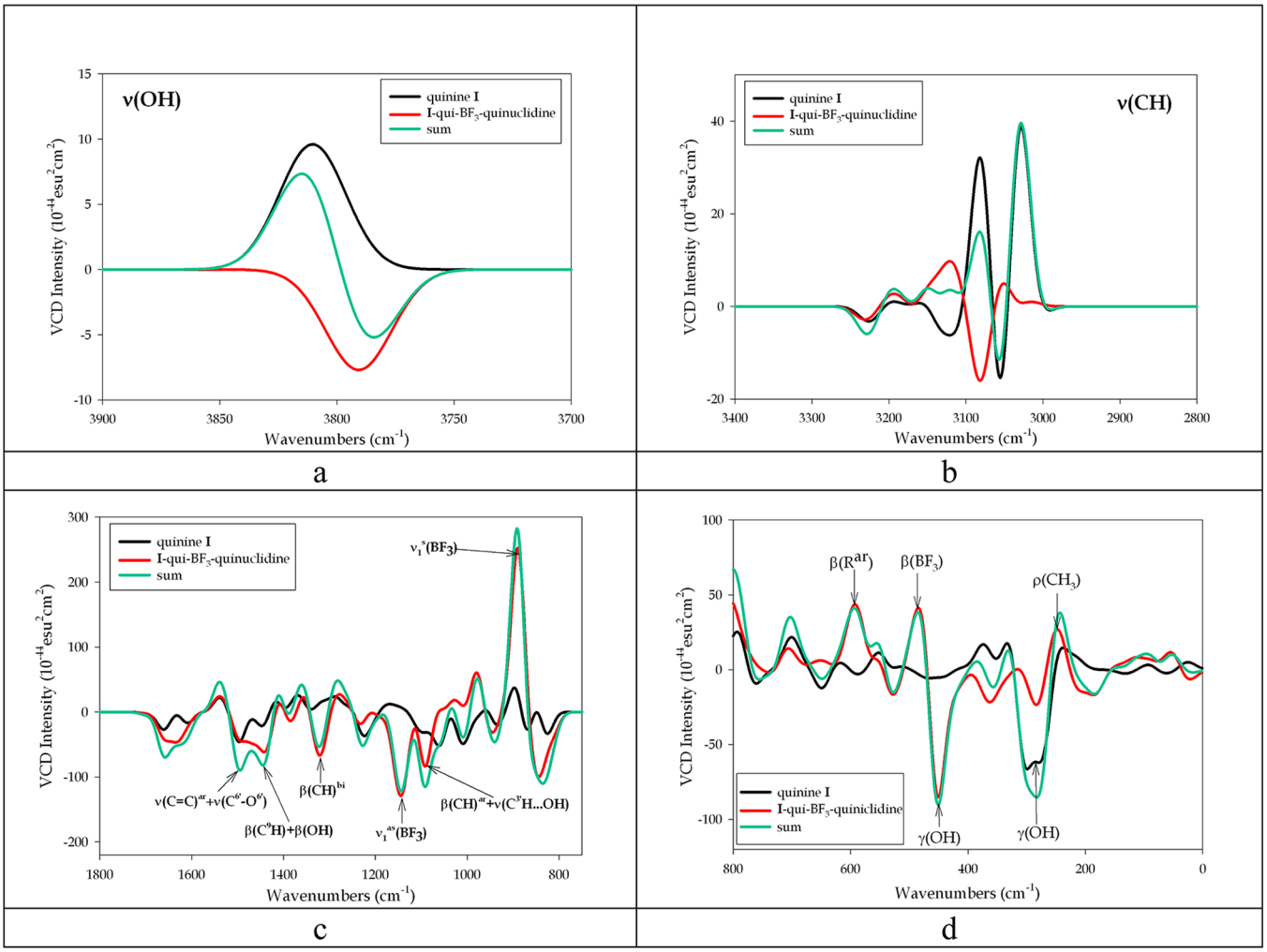

Figure 4. Population-weighed B3LYP/aug-cc-pVDZ VCD spectra of quinine conformer **I** and its most stable **I**-qui-BF_3-quinuclidine complex. The superposition of the two spectra is presented by the green line to show possible mutual compensations between bands of the reagent and the complex.

quinuclidine complex changed by the intermolecular O–H···F–B hydrogen bond with the H···F distance of 2.123 Å (Figure 2).

3.3. Calculated VCD Spectra of the Quinine···BF_3 Complexes. The entire VCD spectra of quinine and its BF_3 complexes calculated at the B3LYP/aug-cc-pVDZ level are gathered in Table 7SI in Supporting Information. Here, only the spectral features characteristic for complex formation, differentiating the complexes, and revealing the chirality transfer phenomena are commented. Although in principle the 2000–800 cm^{-1} range of the VCD spectra is registered, the remaining parts of the calculated VCD spectra for quinine and its four complexes are also presented in Figures 3 and 4. In Figure 3 the spectra of the mixture components are unweighted by population factors, whereas in Figure 4 the ΔG-based Boltzmann factors (Table 3) reduce the system to a binary one: the most stable quinine conformer **I** and the most stable complex of **I** with BF_3 (**I**-qui-BF_3-quinuclidine).

Along with the VCD spectra we also calculated, analyzed, and interpreted the classical mid-IR spectra of the studied systems. The analysis of IR spectra leads to elucidation of spectral patterns indicative of quinine···BF_3 complex formation, allowing for thorough examination of this very system (Figure 2SI, Supporting Information). However, we skip analysis of the classical IR spectra as introducing relatively little novelty to current knowledge on manifestation of EDA complexes in the IR spectra. On the contrary, we focus on manifestation of EDA in the VCD spectra as VCD is a relatively new technique and the influence of EDA complex formation on VCD spectra was studied in only one paper.[39] Therefore, the influence of the intermolecular interactions, and especially EDA complex formation, on VCD spectra needs to be investigated, understood, and explored to be well recognized for future applications of VCD spectra to practical problems.

3.3.1. Unweighted VCD Spectra. The unweighted VCD spectra of quinine monomer and the four complexes are presented in Figure 3. First notice that in the OH stretching vibration band of quinine itself and of the **I**-qui-BF_3-quinoline, **I**-qui-BF_3-OH, and **I**-qui-BF_3-methoxy complexes is positive, whereas that of the most stable **I**-qui-BF_3-quinuclidine complex is negative (Figure 3a). This is due to the additional stabilization of the **I**-qui-BF_3-quinuclidine complex by the O–H···F–B hydrogen bond present only in this complex. Nevertheless, the OH stretching vibration region is registered by a minority of spectrometers and the OH bands are likely to be broad and hardly diagnostic. Thus, the OH range is hardly significant as a marker region. The feature worth noticing is that

dx.doi.org/10.1021/jp304955v | J. Phys. Chem. A 2012, 116, 7916–7926

the VCD intensities in complexes are usually larger than that of quinine alone.

The VCD bands in the CH stretching vibration range, around 3000 cm^{-1} (Figure 3b), are not valuable for discriminating the complexes because of a multitude of mutually overlapping bands of all complexes. Again, this range is also not covered by typical VCD accessory. The unweighted VCD spectra in the fingerprint region (Figure 3c,d) show first and foremost the strong bands characteristic for the **I**-qui-BF_3-quinuclidine complex, whereas there would be some exceptional possibilities for selective identification of the remaining complexes if they could be populated enough in the mixture (Table 3).

3.3.2. Weighted VCD Spectra. The B3LYP/aug-cc-pVDZ calculations show that in practice **I**-qui-BF_3-quinuclidine is the only complex present in the mixture (Table 3). Based on interaction energy, the presence of uncomplexed quinine (in the gas phase) is very unlikely (Table 3); however, because in solution the complexation equilibria may be shifted more toward uncomplexed species, in Figure 4 the spectra of both quinine and the most stable complex with BF_3 are juxtaposed. The superposition of the two spectra, quinine and **I**-qui-BF_3-quinuclidine, is presented in green to show possible mutual compensations between the reagent and the complex (Figure 4).

Quinine and the **I**-qui-BF_3-quinuclidine complex exhibit the OH stretching vibration VCD bands of opposite signs, which maxima are separated by ca. 20 cm^{-1} (Figure 4a). Therefore, if they would not be very broad, a sigmoidal pattern could be observed in this range. Such a pattern would indicate which of the two species is dominating. However, reliable VCD measurements of this region are hardly possible. In the range of 3300−2800 cm^{-1}, the VCD bands of quinine and the **I**-qui-BF_3-quinuclidine complex are likely to be either overlapped or compensated and thus it is hardly discriminative for the complex (Figure 4b).

The VCD spectra in the fingerprint range (1800−200 cm^{-1}) allow for detection and characterization of the intermolecular **I**-qui-BF_3-quinuclidine complex (Figure 4c,d). The chirality transfer modes that possibly can be detected in the VCD spectrum are positioned at 1148 and 885 cm^{-1} (Figure 4c). They can be assigned to the asymmetric $\nu_1^{as}(BF_3)$ stretching and symmetric $\nu^s(BF_3)$ stretching vibration bands, respectively. The $\nu^s(BF_3)$ mode has a large contribution from the ν(B···N) intermolecular stretching vibrations mode. In terms of PED contributions[61] of the vibrational modes of the complex, the former conserves ca. 50% and the latter ca. 60% of the pure vibration present in the uncomplexed BF_3 molecule (Table 4). The former has a negative sign and is relatively strong (−107 × 10^{-44} $esu^2{\cdot}cm^2$), whereas the latter is the strongest in the whole VCD spectrum and is positive (173 × 10^{-44} $esu^2{\cdot}cm^2$). Two other bands of the complex contribute to the band at ca. 885 cm^{-1}, which makes the band even more intense. Also, two other medium-intensity negative bands (at 1139 and 1126 cm^{-1}) contribute to the band at ca. 1148 cm^{-1}. The other chirality transfer modes [1109 cm^{-1} $\nu_2^{as}(BF_3)$; 613 and 608 cm^{-1} umbrella $\delta(BF_3)$ mode(s); 488 and 487 cm^{-1} bending $\beta(BF_3)$ mode] are predicted to be either too weak or compensated and thus probably cannot be recognized in the VCD spectrum (Figure 4c,d).

Sheer identification of the complex based on marker bands for the complex also can be performed by observation of the bands at 1320 cm^{-1} (−56 × 10^{-44} $esu^2{\cdot}cm^2$); 1095 cm^{-1} (−119 × 10^{-44} $esu^2{\cdot}cm^2$); 981 cm^{-1} (60 × 10^{-44} $esu^2{\cdot}cm^2$); 835 cm^{-1} [a superposition of three bands of intensity equal to (−45, −52, and −30) × 10^{-44} $esu^2{\cdot}cm^2$]; 608 cm^{-1} [a superposition of two bands of intensity equal to (27 and 38) × 10^{-44} $esu^2{\cdot}cm^2$]; 468 cm^{-1} (62 × 10^{-44} $esu^2{\cdot}cm^2$); and 456 cm^{-1} (−117 × 10^{-44} $esu^2{\cdot}cm^2$). The latter two bands are very characteristic ones and are due to out-of-plane vibrations of the O−H···F−B moiety (Figure 4d).

Table 4. Comparison of B3LYP/aug-cc-pVDZ Frequencies, IR Intensities, Rotational Strengths, and ζ-Ratio Robustness Measures[a] of Chirality Transfer Modes in the I-qui-BF_3-Quinuclidine Complex[b]

mode	freq (cm^{-1})	IR int (km/mol)	R (10^{-44} $esu^2{\cdot}cm^2$)	ζ-ratio (ppm)	assignment and PED
$\nu_1^{as}(BF_3)$	1148	290	−108	−11	51% $\nu_1^{as}(BF_3)$
$\nu_2^{as}(BF_3)$	1109	168	52	9	55% $\nu_2^{as}(BF_3)$ + 10% $\beta_2(BF_3)$
$\nu^s(BF_3)$	885	194	173	20	60% $\nu^s(BF_3)/\nu$(B···N) + 10% $\delta(BF_3)$
$\delta(BF_3)$	613	21	−17	−13	36% $\delta(BF_3)$[c]
$\delta(BF_3)$	608	16	27	25	21% $\delta(BF_3)$[c]
$\beta_1(BF_3)$	488	3	19	83	38% $\beta_1(BF_3)$ + 11% $\nu_1^{as}(BF_3)$
$\beta_2(BF_3)$	487	6	7	14	52% $\beta_2(BF_3)$ + 13% $\nu_1^{as}(BF_3)$

[a]Góbi and Magyarfalvi.[84,86] [b]Only modes with PED contributions exceeding 10% are considered. [c]Because the size of the system, even with careful PED analysis, for some bands one can select only one mode with a significant contribution and the contributions of the other local modes are meaningless (below 10%). This is the case for vibrations at 613 and 608 cm^{-1}, where only BF_3 out-of-plane deformations are significant.

The band at 1095 cm^{-1} of −119 × 10^{-44} $esu^2{\cdot}cm^2$ VCD intensity is due to combination of the aromatic CH bending vibrations with a contribution of the aromatic $C^{2'}-C^{3'}$ stretching vibrations. It seems that an important element of this complex vibration is due to H···O strength in the $C^{3'}H\cdots O^9-H$ intramolecular hydrogen bond.

3.3.3. Chirality Transfer in Quinine··· BF_3 Complexes. The key problem of VCD intensity calculations in general and the intensity of chirality transfer bands in particular is the reliability of the computational prediction. The first concept for determination of robustness of the VCD intensity, proposed by Nicu et al.,[81−83] was shown to be strongly gauge-dependent.[84,85] Góbi and Magyarfalvi[84,86] have recently proposed an alternative dimensionless and gauge-independent criterion of the VCD mode robustness defined as ratio ζ of the rotational and dipole strengths: $\zeta = R_i/D_i$. According to them, the mode is robust when ζ exceeds 10 ppm. Moreover, few experimental papers showed that VCD features could reliably be detected experimentally even if they are classified as nonrobust.[84,86] Also, it was found that, depending on the experimental systems, the reliability limit of 10 ppm can be even decreased.[87]

Quite recently we have demonstrated that the shape of the potential energy surface (PES) of some chirality transfer modes is also of importance.[39] Namely, we have shown that certain of the chirality transfer modes are stable under slight geometrical changes of the complex about the equilibrium structure while unstable under the other changes. Moreover, the same parent mode of an achiral molecule can be robust when the molecule

dx.doi.org/10.1021/jp304955v | J. Phys. Chem. A 2012, 116, 7916−7926

is bound to one interaction site whereas nonrobust when it is attached to the other site. Therefore, conclusions formulated on the basis of one system cannot be directly transferred even to a quite similar one. So, a simple and universal measure of reliability of the VCD modes can hardly be formulated for chirality transfer modes.

The mode robustness seems to be of great importance, especially in selecting the proper bands for comparison of experimental and theoretical spectra to determine the absolute configuration, to correctly identify molecular conformation, and to reliably scale the theoretical method for VCD calculations. However, when the aim of VCD observations is to monitor changes of the VCD intensities, one must accept the possibility that VCD mode may alter and may transform from being robust to nonrobust or vice versa. Nevertheless, it seems rational to always check whether the calculated chirality transfer modes are robust or not.

Out of two chirality transfer modes of the **I**-qui-BF_3-quinuclidine complex, $\nu_1^{as}(BF_3)$ and $\nu^s(BF_3)/\nu(B\cdots N)$ at 1148 and 885 cm^{-1}, the former mode is nonrobust but the latter one is definitely robust (ζ = 19.8, Table 4).[84,86]

The $\nu_2^{as}(BF_3)$ chirality transfer mode at 1109 cm^{-1} is nonrobust (Table 7SI, Supporting Information), and despite this fact it would disappear from the VCD spectrum because of mutual compensation with the neighboring bands when the widths are not sufficiently narrow. According to the ζ-ratio criterion, the umbrella $\delta(BF_3)$ modes at 613 and 608 cm^{-1} and the bending $\beta(BF_3)$ modes at 488 and 487 cm^{-1} are robust (Table 4). However, at the bandwidth of ca. 15 cm^{-1}, the bands near 600 cm^{-1} are overlapped with the band at ca. 590 cm^{-1}, yielding one contour of positive sign. This problem probably can be solved by using the MI-VCD technique.[12] Thus, despite robustness, the usefulness of this range to monitor the chirality transfer phenomenon in standard conditions is vague. Finally, the bending chirality transfer modes below 500 cm^{-1} are too weak to be used as marker bands (Figure 4d).

Last but not least, an issue that cannot be ignored when the mode robustness is analyzed is conservation of the parent character of the mode upon complexation. The stronger the interaction, the more the mode can lose its parent identity. Thus it is desirable to check somehow the degree of mode identity upon complexation to say that the mode in the complex can be assigned to the moiety that was achiral in the absence of interaction. As we have shown recently, the well-recognized potential energy distribution (PED) procedure can be one of the methods helping with mode identity verification.[39] According to the PED routine, the chirality transfer modes studied here conserved the original character in at least 50% (Table 4). Let us finally stress that, based on our previous[39] and current studies, the dominant factor in VCD activity of previously achiral molecules is the presence of the field of the chiral molecule connected to the degree of molecular asymmetry. Indeed, even for very weak interactions of BF_3 or CO_2 with a chiral substance, in which the achiral molecule is almost undeformed, some of the chirality transfer VCD bands may exhibit significant VCD activity. On the other hand, in strong BF_3 complexes,[39] the molecule is pyramidal, the degeneracy of its modes is released, and the chiral molecule modes are mixed with those of the achiral moiety and contribute to the intensity of the chirality transfer modes. However, the above two factors influencing the VCD chirality transfer band intensity are hardly separable from each other.

In conclusion of this section, we can state that at least one chirality transfer band is robust and is indicative for the chirality transfer phenomenon. However, general rules suggesting the VCD intensity trends when EDA complexes are formed remain unknown so far. Therefore, much more computational and experimental study is needed to understand the chirality transfer phenomenon in EDA complexes.

4. CONCLUSIONS

When a chiral molecule interacts with an achiral one, the latter becomes VCD-visible. This phenomenon, called chirality transfer, was several times reported for hydrogen bond intermolecular complexes, while for electron donor−acceptor (EDA) complexes it is almost unknown. In this paper, we continue investigating the VCD chirality transfer phenomenon in the case of intermolecular EDA quinine$\cdots BF_3$ complexes. To this aim, the conformational landscape of quinine was first explored at the B3LYP/cc-pVDZ level, and for the 14 most stable geometries the calculations were repeated at the B3LYP/aug-cc-pVDZ level. Considerable agreement between X-ray data and the most stable conformer geometries was achieved.

Next, for the most stable quinine conformer, we studied the quinine EDA complexes with BF_3 attached to each of the four quinine electron donor sites: two nitrogen atoms in the aromatic quinoline and aliphatic quinuclidine rings, and two oxygen atoms of the alcohol and methoxy groups. Four principal intermolecular quinine$\cdots BF_3$ complexes were found for the most stable quinine conformer. The complexes interacting via the N atoms are more stable than those via the O atoms by ca. 20 kcal/mol. The complex formed through the tertiary aliphatic quinuclidine N atom is definitely dominating in the system, as it is more stable by ca. 4−6 kcal/mol than that formed through the aromatic quinoline N atom.

The VCD spectra calculated for the quinine$\cdots BF_3$ complexes at the B3LYP/aug-cc-pVDZ level reveal the chirality transfer modes. For the most stable quinine$\cdots BF_3$ complex dominating in the mixture, one of the chirality transfer modes at 885 cm^{-1}, assigned to $\nu^s(BF_3)$ symmetric stretching vibrations with significant contribution of the $\nu(B\cdots N)$ intermolecular stretching vibrations, is the most intense in the entire VCD spectrum. Also, since it is robust according to Góbi and Magyarfalvi robustness criterion, it is indicative for the chirality transfer phenomenon. The other chirality transfer modes, $\nu_1^{as}(BF_3)$, $\nu_2^{as}(BF_3)$, umbrella $\delta(BF_3)$, and bending $\beta(BF_3)$, are discussed in detail in the context of their diagnosticity and robustness.

Summing up, it was shown that the VCD chirality transfer phenomenon can be observed for EDA complexes. Moreover, some of the chirality transfer modes meet criteria of mode robustness and are definitely diagnostic for the phenomenon. However, the general rules that govern the trends of VCD intensity of the EDA complexes remain unknown. Therefore, much more computational and experimental study is needed to understand the chirality transfer phenomenon in EDA complexes.

■ ASSOCIATED CONTENT

Supporting Information

Seven tables and two figures with detailed energetics, geometry, Cartesian coordinates, frequency details, structures presented in the paper, and IR spectra of the quinine$\cdots BF_3$ EDA complexes.

This material is available free of charge via the Internet at http://pubs.acs.org.

AUTHOR INFORMATION

Corresponding Author

*E-mail rzepka@icm.edu.pl; tel +48-22-568-24-21; fax +48-22-568-22-93.

Notes

The authors declare no competing financial interest.

E-mail Joanna.Rode@ichp.pl (J.E.R., alt); micjam@wp.pl (M.H.J.); janek@il.waw.pl (J.Cz.D.); sadlej@chem.uw.edu.pl (J.S.).

ACKNOWLEDGMENTS

This work was financially supported by ICRI (Warsaw) within the framework of statutory activity. Partial support from Grant N N204 443 140 from National Science Centre in Poland is gratefully acknowledged. The computational G19-4 grant from the Interdisciplinary Center of Mathematical and Computer Modeling (ICM) at Warsaw University is acknowledged for a generous allotment of computer time.

REFERENCES

(1) Holzwarth, G.; Hsu, E. C.; Mosher, H. S.; Faulkner, T. R.; Moscowitz, A. *J. Am. Chem. Soc.* **1974**, *96*, 251−252.

(2) Nafie, L. A.; Cheng, J. C.; Stephens, P. *J. Am. Chem. Soc.* **1975**, *97*, 3842−3843.

(3) Nafie, L. A.; Keiderling, T. A.; Stephens, P. J. *J. Am. Chem. Soc.* **1976**, *98*, 2715−2723.

(4) Sugeta, H.; Marcott, C.; Faulkner, T. R.; Overend, J.; Moscovitz, A. *Chem. Phys. Lett.* **1976**, *40*, 397−398.

(5) Ostrowski, S.; Jamróz, M. H.; Rode, J. E.; Dobrowolski, J. Cz. *J. Phys. Chem. A* **2012**, *116*, 631−643.

(6) Nafie, L. A. Polarization Modulation FTIR Spectroscopy. In *Advances in Applied FTIR Spectroscopy*; Mackenzie, M. W., Ed.; John Wiley and Sons: New York, 1988; pp 67−104.

(7) Nafie, L. A.; Dukor, R. K.; Freedman, T. B. Vibrational Circular Dichroism. In *Handbook of Vibrational Spectroscopy*; Chalmers, J. M., Griffiths, P. R., Eds.; John Wiley & Sons Ltd.: Chichester, U.K., 2002; pp 731−744.

(8) Pecul, M.; Ruud, K. *Adv. Quantum Chem.* **2005**, *50*, 185−212.

(9) Stephens, P. J.; Delvin, F. J. *Chirality* **2000**, *12*, 172−179.

(10) Devlin, F. J.; Stephens, P. J.; Österle, C.; Wiberg, K. B.; Cheeseman, J. R.; Frisch, M. J. *J. Org. Chem.* **2002**, *67*, 8090−8096.

(11) Freedman, T. B.; Cao, X.; Dukor, R. K.; Nafie, L. *Chirality* **2003**, *15*, 743−758.

(12) Tarczay, G.; Magyarfalvi, G.; Vass, E. *Angew. Chem.* **2006**, *45*, 1775−1777.

(13) Freedman, T. B.; Cao, X.; Phillips, L. M.; Cheng, P. T. W.; Dalterio, R.; Shu, Y.-Z.; Zhang, H.; Zhao, N.; Shukla, R. B.; Tymiak, A.; Gozo, S. K.; Nafie, L. A.; Gougoutas, J. Z. *Chirality* **2006**, *18*, 746−753.

(14) Monde, K.; Miura, N.; Hashimoto, M.; Taniguchi, T.; Inabe, T. *J. Am. Chem. Soc.* **2006**, *128*, 6000−6001.

(15) Debie, E.; Bultinck, P.; Herrebout, W.; van der Veken, B. *Phys. Chem. Chem. Phys.* **2008**, *10*, 3498−3508.

(16) Sadlej, J.; Dobrowolski, J. Cz.; Rode, J. E. *Chem. Soc. Rev.* **2010**, *39*, 1478−1488.

(17) Dobrowolski, J. Cz.; Rode, J. E.; Sadlej, J. VCD Chirality Transfer: a New Insight into the Intermolecular Interactions. in *Practical Aspects of Computational Chemistry I. An Overview of the Last Two Decades and Current Trends*; Leszczynski, J.; Shukla, M. K., Eds.; Springer: Dordrecht, Heidelberg, London, New York, 2012; pp 451−477.

(18) Burgi, T.; Vargas, A.; Baiker, A. *J. Chem. Soc., Perkin Trans.* **2002**, *2*, 1596−1601.

(19) Rode, J. E.; Dobrowolski, J. Cz. *J. Mol. Struct. (THEOCHEM)* **2003**, *637*, 81−89.

(20) Sadlej, J.; Dobrowolski, J. Cz.; Rode, J. E.; Jamróz, M. H. *Phys. Chem. Chem. Phys.* **2006**, *8*, 101−113.

(21) Sadlej, J.; Dobrowolski, J. Cz.; Rode, J. E.; Jamróz, M. H. *J. Phys. Chem. A* **2007**, *111*, 10703−10711.

(22) Kuppens, T.; Herrebout, H.; van der Veken, B.; Bultinck, P. *J. Phys. Chem. A* **2006**, *110*, 10191−10200.

(23) Debie, E.; Jaspers, L.; Bultinck, P.; Herrebout, W.; van der Veken, B. *Chem. Phys. Lett.* **2008**, *450*, 426−430.

(24) Aviles-Moreno, J. R.; Urena Horno, E.; Partal Urena, F.; López González, J. J. *Spectrochim Acta A* **2011**, *79*, 767−776.

(25) Merten, C.; Amkreutz, M.; Hartwig, A. *Phys. Chem. Chem. Phys.* **2010**, *12*, 11635−11641.

(26) Losada, M.; Xu, Y. *Phys. Chem. Chem. Phys.* **2007**, *9*, 3127−3135.

(27) Sun, W.; Wu, J.; Zheng, B.; Zhu, Y.; Liu, C. *J. Mol. Struct. (THEOCHEM)* **2007**, *809*, 161−169.

(28) Losada, M.; Tran, H.; Xu, Y. *J. Chem. Phys.* **2008**, *128*, No. 014508.

(29) Losada, M.; Nguyen, P.; Xu, Y. *J. Phys. Chem. A* **2008**, *112*, 5621−5627.

(30) Yang, G.; Xu, Y. *J. Chem. Phys.* **2009**, *130*, No. 164506.

(31) Liu, Y.; Yang, G.; Losada, M.; Xu, Y. *J. Chem. Phys.* **2010**, *132*, No. 234513.

(32) Tarczay, G.; Góbi, S.; Vass, E.; Magyarfalvi, G. *Vib. Spectrosc.* **2009**, *50*, 21−28.

(33) Meyer, E. A.; Castellano, R. K.; Diederich, F. *Angew. Chem., Int. Ed.* **2003**, *42*, 1210−1250.

(34) Korolkovas, A. *Essentials of Medical Chemistry*, 2nd ed.; Wiley, New York, 1998; Chapt. 3.

(35) Takahasi, K.; Horino, K.; Komura, T.; Murata, K. *Bull. Chem. Soc. Jpn.* **1993**, *66*, 733−738.

(36) Andrade, S. M.; Costa, S. M. B.; Pansu, R. *J. Colloid Interface Sci.* **2000**, *226*, 260.

(37) Slifkin, A. M. *Charge−Transfer Interaction of Biomolecules*; Academic Press: New York, 1971.

(38) Abou Attia, F. M. *Farmaco* **2000**, *55*, 659−664.

(39) Rode, J. E.; Dobrowolski, J. Cz. *Chirality* **2012**, *24*, 5−16.

(40) Jeon, Y. J.; Bharadwaj, P. K.; Choi, S.; Lee, J. W.; Kim, K. *Angew. Chem., Int. Ed.* **2002**, *41*, 4474−4476.

(41) Kulinowski, K.; Gould, I. R.; Myers, A. B. *J. Phys. Chem.* **1995**, *99*, 9017−9026.

(42) Jamróz, M. H.; Dobrowolski, J. Cz.; Bajdor, K.; Borowiak, M. A. *J. Mol. Struct.* **1995**, *349*, 9−12.

(43) Dobrowolski, J. Cz.; Jamróz, M. H. *J. Mol. Struct.* **1992**, *267*, 211−219.

(44) Besnard, M.; Isabel Cabacüo, M.; Longelin, S.; Tassaing, T.; Danten, Y. *J. Phys. Chem. A* **2007**, *111*, 13371−13379.

(45) Meredith, J. C.; Johnston, K. P.; Seminario, J. M.; Kazarian, S. G.; Eckert, C. A. *J. Phys. Chem.* **1996**, *100*, 10837−10848.

(46) Legon, A. C.; Lister, D. G.; Thorn, J. C. *J. Chem. Soc., Faraday Trans.* **1994**, *90*, 3205−3212.

(47) Dobrowolski, J. Cz.; Kawęcki, R. *J. Mol. Struct.* **2005**, *734*, 235−239.

(48) Song, C. E. An Overview of Cinchona Alkaloids in Chemistry. In *Cinchona Alkaloids in Synthesis and Catalysis, Ligands, Immobilization and Organocatalysis*; Song, C. E., Ed.; Wiley−VCH Verlag: Weinheim, Germany, 2009.

(49) Sheldon, R. A. *Chirotechnology*; Marcel Dekker: New York, 1993.

(50) Valentine, R. Enantiomeric Resolution of Racemic Ibuprofen in Supercritical Carbon Dioxide Using a Chiral Resolving Agent. Ph.D. Dissertation, University of Pittsburgh, Pittsburgh, PA, 2002.

(51) *The Hydrogen Bond: Recent Developments in Theory and Experiments*, Vols. *1*−*3*; Schuster, P., Zundel, G., Sandorfy, C., Eds.; North-Holland Elsevier: Amsterdam, 1976.

(52) Becke, A. D. *J. Chem. Phys.* **1993**, *98*, 5648−5652.

(53) Burke, K.; Perdew, J. P.; Wang, Y. *Electronic Density Functional Theory: Recent Progress and New Directions*; Dobson, J. F., Vignale, G., Das, M. P., Eds.; Plenum: New York, 1998.
(54) Janoschek, R. *Pure Appl. Chem.* **2001**, *73*, 521−1553.
(55) Dunning, T. H., Jr. *J. Chem. Phys.* **1989**, *90*, 1007−1023.
(56) Kendall, R. A.; Dunning, T. H.; Harrison, R. J. *J. Chem. Phys.* **1992**, *96*, 6796−6806.
(57) Boys, S. F.; Bernardi, F. *Mol. Phys.* **1970**, *19*, 553−566.
(58) Turi, L.; Dannenberg, J. J. *J. Phys. Chem.* **1993**, *97*, 2488−2490.
(59) Rode, J. E.; Dobrowolski, J. Cz. *Chem. Phys. Lett.* **2002**, *360*, 123−132.
(60) Frisch, M. J.; Trucks, G. W.; Schlegel, H. B.; Scuseria, G. E.; Robb, M. A.; Cheeseman, J. R.; Scalmani, G.; Barone, V.; Mennucci, B.; Petersson, G.; et al. Gaussian 09, Revision A.1; Gaussian, Inc., Wallingford CT, 2009.
(61) Jamróz, M. H. Vibrational Energy Distribution Analysis VEDA 4 Program, Warsaw,Poland, 2004−2010.
(62) Jamróz., M. H.; Dobrowolski, J. Cz.; Brzozowski, R. *J. Mol. Struct.* **2006**, *787*, 172−183.
(63) Keresztury, G.; Jalsovszky, G. *J. Mol. Struct.* **1971**, *10*, 304−305.
(64) Allen, W. D.; Császár, A. G.; Horner, D. A. *J. Am. Chem. Soc.* **1992**, *114*, 6834−6849.
(65) Chapman, D. M.; Hester, R. E. *J. Phys. Chem. A* **1997**, *101*, 3382−3387.
(66) Dobrowolski, J. Cz.; Ostrowski, S.; Kołos, R.; Jamróz, M. H. *Vib. Spectrosc.* **2008**, *48*, 82−91.
(67) Vargas, A.; Bonalumi, N.; Ferri, D.; Baiker, A. *J. Phys. Chem. A* **2006**, *110*, 1118−1127.
(68) Dijkstra, G. D. H.; Kellogg, R. M.; Wynberg, H. *Recl. Trav. Chim. Pays-Bas* **1989**, *108*, 195−204.
(69) Dijkstra, G. D. H.; Kellogg, R. M.; Wynberg, H.; Svendsen, J. S.; Marko, I.; Sharpless, K. B. *J. Am. Chem. Soc.* **1989**, *111*, 8069−8076.
(70) Dijkstra, G. D. H.; Kellogg, R. M.; Wynberg, H. *J. Org. Chem.* **1990**, *55*, 6121−6131.
(71) Bürgi, T.; Baiker, A. *J. Am. Chem. Soc.* **1998**, *120*, 12920−12926.
(72) Caner, H.; Biedermann, P. U.; Agranat, I. *Chirality* **2003**, *15*, 637−645.
(73) Obaleye, J. A.; Caira, M. R.; Tella, A. C. *J. Chem. Crystallogr.* **2007**, *37*, 707−712.
(74) Suszko-Purzycka, A.; Lipinska, T.; Piotrowska, E.; Oleksyn, B. J. *Acta Crystallogr., Sect. C* **1985**, *41*, 977−980.
(75) Borowiak, T.; Dutkiewicz, G.; Thiel, J. *Z. Naturforsch. B: Chem. Sci.* **2002**, *57*, 586−592.
(76) Boratyński, P. J.; Turowska-Tyrk, I.; Skarzewski, J. *J. Org. Chem.* **2008**, *73*, 7357−60.
(77) Pniewska, B.; Suszko-Purzycka, A. *Acta Crystallogr. Sect. C* **1989**, *45*, 638−642.
(78) Dobrowolski, J. Cz.; Jamróz, M. H.; Kołos, R.; Rode, J. E.; Sadlej, J. *Chem. Phys. Chem.* **2007**, *8*, 1085−1094.
(79) Dobrowolski, J. Cz.; Jamróz, M. H.; Kołos, R.; Rode, J. E.; Sadlej, J. *Chem. Phys. Chem.* **2008**, *9*, 2042−2051.
(80) Dobrowolski, J. Cz.; Jamróz, M. H.; Kołos, R.; Rode, J. E.; Cyrański, M. K.; Sadlej, J. *Phys. Chem. Chem. Phys.* **2010**, *12*, 10818−10830.
(81) Nicu, V. P. Implementation, Calculation and Interpretation of Vibrational Circular Dichroism Spectra. Ph.D Thesis, Vrije Universiteit, Amsterdam, 2009.
(82) Nicu, V. P.; Baerends, E. J. *Phys. Chem. Chem. Phys.* **2009**, *11*, 6107−6118.
(83) Nicu, V. P.; Debie, E.; Herrebout, W.; van der Veken, B.; Bultinck, P.; Baerends, E. J. A *Chirality* **2010**, *21*, E287−E297.
(84) Góbi, S.; Magyarfalvi, G. *Phys. Chem. Chem. Phys.* **2011**, *13*, 16130−16133.
(85) Magyarfalvi, G.; Tarczay, G.; Vass, E. *WIREs Comput. Mol. Sci.* **2011**, *1*, 403−425.
(86) Góbi, S.; Vass, E; Magyarfalvi, G.; Tarczay, G. *Phys. Chem. Chem. Phys.* **2011**, *13*, 13972−13984.
(87) Poopari, M. R.; Dezhahang, Z.; Yang, G.; Xu, Y. *ChemPhysChem* **2012**, *13*, 2310−2321.